ELSEVIER

Thin Solid Films 371 (2000) 114–118

thin solid films

www.elsevier.com/locate/tsf

Texturing of polycrystalline SiC films on graphitic carbon in laminated composites grown by forced-flow chemical vapor infiltration

K.A. Appiah[a], Z.L. Wang[a,*], W.J. Lackey[b]

[a]*School of Materials Science and Engineering, Georgia Institute of Technology, Atlanta, GA 30332-0245, USA*
[b]*School of Mechanical Engineering, Georgia Institute of Technology, Atlanta, GA 30332-0245, USA*

Received 16 January 2000; received in revised form 7 April 2000; accepted 11 April 2000

Abstract

The growth and orientation of SiC on pyrocarbon using forced-flow thermal gradient chemical vapor infiltration to deposit alternate layers of these materials has been examined by transmission electron microscopy. The SiC layers were determined to be predominantly of the cubic (β) polytype, and the close-packed $\{111\}_{SiC}$ planes were found to be mostly oriented parallel and next to the highly dense $\{0001\}_{C}$ basal planes of the pyrocarbon layers at the interface. A model involving close-packed plane sequencing is proposed for the C/SiC interface. © 2000 Elsevier Science S.A. All rights reserved.

Keywords: Carbides; Surface structure; Transmission electron microscopy (TEM)

1. Introduction

Silicon carbide is a versatile material possessing properties such as a wide energy band gap, high thermal conductivity, high elastic modulus and high-temperature creep resistance, which enable it to be used in a wide variety of electronic, optical and structural applications. Also, carbon, in the form of polycrystalline graphite, is well known for it is excellent thermal and electrical properties that enable its use in a variety of applications due to its anisotropic and layered structure. Carbon, when deposited as pyrocarbon by chemical vapor deposition processes, is known to exhibit varied and interesting microstructures. Thus, SiC and carbon, separately and in combination, have enormous utility in materials applications. Carbon and silicon carbide are ideally suited for use as alternate layered laminate materials due to their chemical compatibility, almost equal thermal expansion coefficients, and ease of fabrication by vapor-phase deposition methods. However, published reports on the use of carbon and SiC in combination, in spite of the enormous potential as a viable material system, are rather scarce.

Chemical vapor infiltration (CVI) is a specialized form of chemical vapor deposition (CVD) in which deposition occurs on surfaces within a porous preform, in contrast to deposition onto an external substrate surface as occurs in CVD. Thus, the thermodynamics and kinetics of the CVD process and the effects on the resulting material's microstructure are directly applicable to the CVI process. CVI is especially suited to the deposition of thin layers because it affords better control of layer thickness. In forced-flow thermal-gradient

* Corresponding author. Fax: +1-404-894-9140.
E-mail address: zhong.wang@mse.gatech.edu (Z.L. Wang).

PII: S0040-6090(00)00988-3

chemical vapor infiltration (FCVI), a thermal gradient applied to the preform coupled with the forced flow of reagents reduces total infiltration time.

In contrast to the vapor-phase nucleation and growth of single crystalline materials which has been investigated in detail and is well understood, the evolution of microstructure of polycrystalline materials has not been sufficiently elucidated. During the nucleation and growth of polycrystalline films on substrates during CVD, it has been known that the deposited material may start with nuclei of random orientations [1]. In cases where oriented columnar microstructures have been observed, they have been typically attributed to preferred growth directions, as opposed to definite orientation relationships between deposit and substrate that is characteristic of epitaxial nucleation and growth [2,3]. However, work by others [4] have shown that specific crystallographic orientation relationships, epitaxy, can occur during the polycrystalline CVD of α-SiC on β-SiC substrates. In the present work, the observed interfacial orientation relationship during the growth of polycrystalline SiC on graphitic carbon during FCVI is presented.

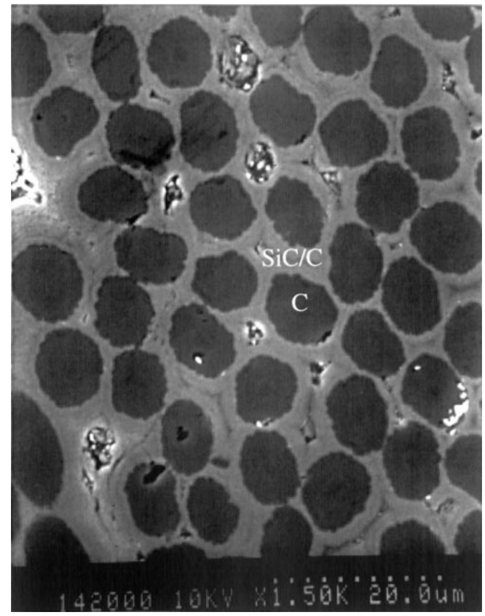

Fig. 1. SEM image showing the distribution of C–SiC layers in the laminate structure. The dark hole-shape contrast areas are the carbon fibers, and the gray contrast areas are the SiC-laminated structures grown around the carbon fibers.

2. Experimental

The alternating layers of carbon and SiC were fabricated by forced-flow thermal-gradient chemical vapor infiltration of fibrous carbon preforms. Details of the FCVI fabrication process, parameters, and reactor configuration have been previously described by Lackey et al. [5]. Briefly, during the FCVI process, the reagent gases are forced to flow through the fibrous carbon preforms, and the reagent streams are altered to deposit the different matrix components alternately. The carbon layers were deposited from a mixture of propylene and hydrogen, whereas the SiC layers were deposited from a mixture of methyltrichlorosilane [MTS] and hydrogen.

Standard procedures for producing thin foils for transmission electron microscopy (TEM) examination were employed. Specimens for TEM examination were obtained by cutting ~1-mm thickness slices from a bulk sample which were then mounted in epoxy, polished, dimpled, and subsequently ion-milled to electron transparency. The ion milling was performed with argon and a rotating cold stage at a voltage of 4 kV. TEM imaging and diffraction and high-resolution TEM (HRTEM) imaging were performed using a JEOL 4000EX high-resolution microscope operating at 400 kV with a point-to-point resolution of 0.18 nm. Both bright-field and dark-field images were recorded using an objective aperture of radius 4 mrad. HRTEM images were recorded using an objective aperture that is large enough to enclose the {0004} reflection of graphite. Scanning electron microscopy (SEM) imaging was performed using a Hitachi S800 FEG machine.

3. Results and discussion

Fig. 1 shows a SEM image of the cross-section of the laminate structure with the central carbon fiber surrounded by radial rings of alternating C and SiC layers. Fig. 2a,b are a pair of bright-field/dark-field TEM images that show the general morphology of the material with alternate layers of pyrocarbon and SiC. The dark-field image was recorded using a dominant diffraction spot indicated by a circle in Fig. 2b. The layers are seen to increase in thickness along the radial growth direction (towards the top of the images). The growth and development of the SiC crystals are evident in the dark-field image of Fig. 2b as small polycrystalline grains that grow directly on top of the carbon layers. The crystal size is seen to be anisotropic, and its length is approximately the thickness of the SiC layer. The selected area electron diffraction pattern from the indicated area in Fig. 2b suggests that the $\{0002\}_{C}$ basal planes of the pyrocarbon layer are parallel and next to the $\{111\}_{SiC}$ planes of the polycrystalline SiC layer. The arcs from the $\{0002\}_{C}$ reflection indicate that the basal planes have a preferred orientation as opposed to random, multiple orientations at the interface. There appears to be a specific orientation relationship, resem-

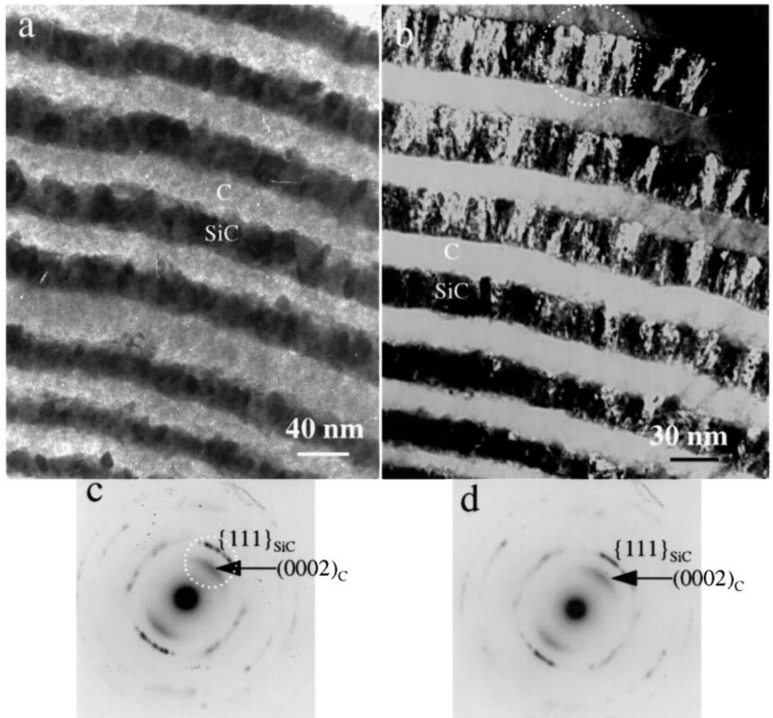

Fig. 2. (a) Bright-field TEM image showing morphology of alternate pyrocarbon and SiC layers. (b) Dark-field TEM image recorded by selecting the reflections enclosed in the circle marked in (c), showing layer morphology and crystallinity of SiC crystals. (c) Electron diffraction patterns recorded from the circled region in (b), showing the parallel orientation of (0002) pyrocarbon planes and the (111) SiC planes. (d) Another electron diffraction recorded from a different location.

bling epitaxy, at least in some localized regions, during the CVI growth of polycrystalline SiC on pyrocarbon.

Fig. 3 is a high-magnification TEM image of the carbon–SiC interface. In this image, growth of the SiC layer occurred on the surface of the pre-existing pyrocarbon layer. It is clear from this high-magnification image that, in some regions, there appears to be a continuity of high-density planes from the pyrocarbon to the SiC layers. This tendency of $\{0001\}_C \parallel \{111\}_{SiC}$ preserves for most of the interfacial regions, consistent with the result from the electron diffraction pattern shown in Fig. 2c, which was recorded from a much larger area. The occurrence of bands or areas which do not seem to exhibit high planar registry (Fig. 3) between

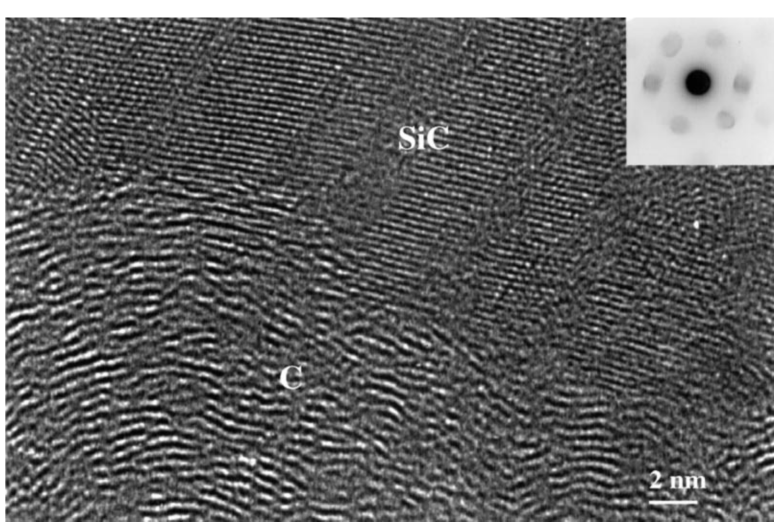

Fig. 3. High-magnification TEM image of carbon–SiC interface showing continuity of high density planes at interface; inset microdiffraction pattern reveals SiC at interface to be β polytype ($\langle 110\rangle_{SiC}$ zone axis/$\{111\}_{SiC}$ reflections).

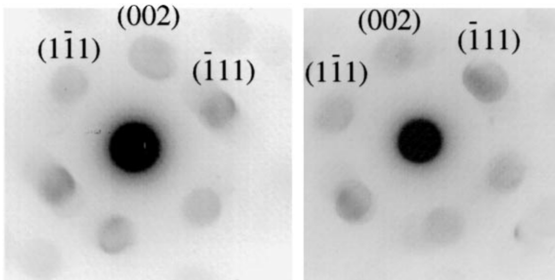

Fig. 4. Typical electron microdiffraction patterns recorded from SiC grains showing its cubic structure.

the areas of seemingly high-density plane continuity could be due to the TEM projection effect of a three-dimensional wavy interface.

The crystal structure of the SiC was determined by electron microdiffraction. Most of the microdiffraction patterns obtained from these interfacial regions were clearly identified to be of the β polytype (13 of 15 or ~ 87%). Examples of such microdiffraction patterns are shown in Fig. 4, which are indexed to be $[110]_{SiC}$ patterns of cubic SiC structure. The small number of microdiffraction patterns from these interfacial regions whose polytype could not be conclusively established appeared to be due to mixed contributions from crystals that have slightly different orientations. The close-packed $\{111\}_{SiC}$ planes of the cubic β-SiC grow directly on top of the highly dense six-membered $\{0001\}_C$ basal planes of the pyrocarbon layer.

β-SiC exhibits the zinc blende structure with interpenetrating face-centered cubic (FCC) lattices of Si and carbon with a relative displacement of $1/4\ [111]_{SiC}$, or, alternatively, a lattice with Si atoms at the fcc positions and carbon atoms occupying one-half of the tetrahedral locations. Thus, the close-packed {111} planes can be viewed as a double layer of Si and carbon atoms, as shown in Fig. 5a. The β-SiC $\{111\}_{SiC}$ planes follow a stacking sequence of ABCABC... The stacking parallel to the basal plane for graphite can be represented by the A′B′A′B′... stacking sequence of the $\{0001\}_C$ planes as shown in Fig. 5b.

The parallel alignment of close-packed planes in the C–SiC system could be explained by considering a simple model of the possible stacking sequence of the close-packed planes at the interface. If the pyrocarbon layer maintains the basal plane at the surface, the next layer of β-SiC $\{111\}_{SiC}$ close-packed planes could easily continue the stacking sequence by occupying the A′, B′ or C′ stacking position (see Fig. 5c), or either of two available positions not occupied by the terminating pyrocarbon layer. The β-SiC $\{111\}_{SiC}$ planes could then easily continue to maintain the ABCABC... stacking sequence characteristic of the cubic close-packed structure. The first contacting layer of β-SiC with C can be either Si or C atoms depending on the energetics of the particular bonding scenario. Such a texturing orientation is likely to exist even at the very first layer of SiC because the carbon fibers at the center tend to have the graphitic layers parallel to the outer surface of the fiber. In this work, such parallel alignment of graphite layers at contacting surfaces may be particularly conducive to the nucleation of SiC $\{111\}_{SiC}$ planes.

Despite the increasing basal plane alignment of the pyrocarbon layer towards the interface, the structure still remains turbostratic and deviant from that of highly crystalline graphite. Crystals of graphite, particularly those deposited from vapor-phase processes are known to exhibit various degrees of preferred orientation of basal planes [6–8] and are mostly turbostratic at low

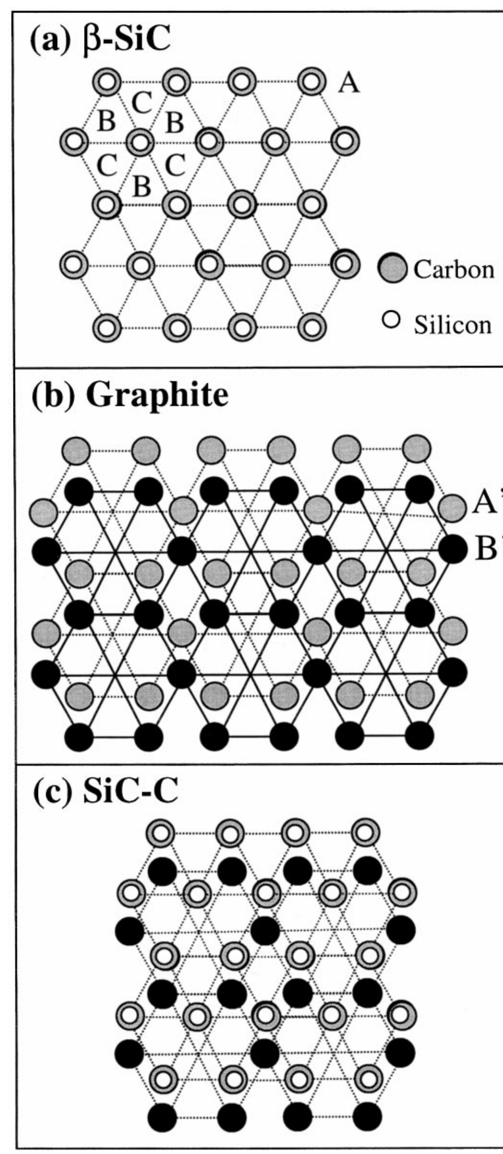

Fig. 5. (a) Model of the ideal stacking sequence of ABCABC... parallel to the β-SiC (111) planes. (b) Model of the ideal stacking sequence, A′B′A′B′..., parallel to the graphite (0001) basal planes. (c) Model of the stacking of high-density planes at the C–SiC interface.

temperatures (approx. 1170 K, similar to the deposition temperature employed in this work). Coupled with the fact that the alternating layers of carbon and SiC are deposited as concentric circles (see Fig. 1), thus introducing some amount of inherent curvature to the interface, it is conceivable that the carbon basal planes would be particularly oriented for favorable nucleation of SiC $\{111\}_{SiC}$ planes only at certain locations. Once nucleation is initiated in these favorable regions, continual growth of the SiC is assured through the layer thickness, hence the array of SiC $\{111\}_{SiC}$ planes emanating from the carbon layer. The SiC grain tends to grow along the radial direction, but the lateral grain size is strongly affected by the curvature of the SiC layer. The dark-field image given in Fig. 2b indicates that the lateral grain size increases with the increase of the radial distance from the central region. This is understandable because the curvature of the layer can be accommodated by the rotation of the grains and the rotation angle increases with a decrease in the radial distance, possibly leading to smaller lateral size.

At the pyrocarbon–SiC interface, the close-packed {111} SiC planes can be stacked on top of the graphite basal planes, such that the $\langle -1\ 1\ 0\rangle_{SiC}$ close-packed direction is parallel to the $\langle 1\ 1\ -2\ 0\rangle_{C}$ direction in the graphite basal plane. Along the close-packed direction in the SiC {111} plane, the interatomic distance is calculated to be ~ 0.308 nm. In the graphite basal planes, the C–C distance is 0.142 nm for nearest neighbors and 0.246 nm for second nearest neighbors. The lattice mismatch, f, was calculated as $d_{SiC}/d_{C} - 1$, where d_{SiC} and d_{C} are the interatomic distances along the pertinent directions in SiC and graphite (second nearest neighbor), respectively. Thus, the calculated lattice mismatch along the $\langle -1\ 1\ 0\rangle_{SiC} \parallel \langle 1\ 1\ -2\ 0\rangle_{C}$ direction is found to be quite large: approximately 0.25. Although the materials were deposited at ~ 1150 K, the thermal expansion effects were not considered in the mismatch calculations because they are not expected to significantly alter the results.

In view of the substantial lattice mismatch and dissimilar crystal structures of the pyrocarbon and SiC layers, some level of localized epitaxy seems to exist at all in this polycrystalline system. Epitaxy has been observed in some systems despite large differences in lattice parameters and crystalline structures such as AlN on Al_2O_3 [9] and CdTe on GaAs [10]. It is believed that localized epitaxy can occur on the individual grains of a polycrystalline substrate, and, furthermore, face-centered cubic (fcc) and hexagonal close-packed (hcp) systems have been known to allow epitaxy on $\{111\}_{SiC}$ and $\{0001\}_{C}$ planes respectively [10]. Such a scenario would be consistent with the apparent localized epitaxy of SiC on graphitic carbon observed in this work. In this work, certain grains of the polycrystalline SiC, namely grains that present $\{111\}_{SiC}$ planes, seem to adopt an epitaxial relationship on the $\{0001\}_{C}$ graphitic basal planes.

In summary, alternating layers of pyrocarbon and SiC were deposited by the FCVI process, and the interface between pyrocarbon and SiC layers were investigated. In some localized areas, there appeared to be a definite orientational relationship between the pyrocarbon layers and the crystalline grains of the SiC layers. In particular, high-magnification TEM and diffraction revealed that highest-density planes seemed to be continuous from the {0001} basal planes of the pyrocarbon layer to the close-packed {111} planes of β-SiC. A simple model of close-packed plane stacking sequence at the interface was proposed and appeared to be consistent with the interfacial observations.

Acknowledgements

KAA thanks the support of Packard fellowship. Research was part supported by NSF grant (DMR-9632823).

References

[1] J.L. Kenty, J.P. Hirth, Surf. Sci. 15 (1969) 403.
[2] A. van der Drift, Philips Res. Rep. 22 (1967) 267.
[3] E.A. Matson, S.A. Polyakov, Phys. Status Solidi A 41 (1997) K93.
[4] B.W. Sheldon, T.M. Besmann, K.L. More, T.S. Moss, J. Mat. Res. 8 (1993) 1086.
[5] W.J. Lackey, S. Vaidyaraman, K.L. More, J. Am. Cer. Soc., 1 80 (1997) 113.
[6] J.D. Buckley, D.D. Edie, Carbon–Carbon Materials and Composites, Noyes Publications, New Jersey, 1993.
[7] A.S. Johansson, J. Lu, J.O. Carlsson, Thin Solid Films 252 (1994) 19.
[8] J. Bokros, in: P.L. Walker (Ed.), Chemistry and Physics of Carbon, 5 (1969) 1.
[9] F.A. Ponce, D.P. Bour, Nature 386 (1997) 351.
[10] D.L. Smith, Thin Film Deposition: Principles and Practice, McGraw-Hill Press, New York, 1995.